NASA Technical Paper 2007

AVRADCOM Technical Report 82-C-4

June 1982

AD A116108

Multiroller Traction Drive Speed Reducer Evaluation for Automotive Gas Turbine Engine

Douglas A. Rohn,
Neil E. Anderson

DTIC

NASA
Technical
Paper
2027

AVRADCOM
Technical
Report
81-C-11

1982

(2)

Multiroller Traction Drive Speed Reducer

Evaluation for Automotive Gas Turbine Engine

Douglas A. Rohn
Lewis Research Center
Cleveland, Ohio

Neil E. Anderson
Propulsion Laboratory
AVRADCOM Research and Technology Laboratories
Lewis Research Center
Cleveland, Ohio

Stuart H. Loewenthal
Lewis Research Center
Cleveland, Ohio

NASA
National Aeronautics
and Space Administration

Scientific and Technical
Information Branch

SUMMARY

Parametric tests were conducted on a nominal 14:1 fixed-ratio Nasvytis multiroller traction drive speed reducer retrofitted to an automotive gas turbine engine. The test drive's sun roller assembly was equipped with a mechanism to proportionately load the rollers in response to the torque on the drive. The gas turbine engine's power turbine assembly was modified to accommodate the Nasvytis drive in place of the single-mesh, 9.69:1 ratio helical gearset. The traction drive and the power turbine support bearings were lubricated by a synthetic, cycloaliphatic traction fluid. The effects of speed and torque on drive power loss, efficiency, creep rate, temperature distribution, and loading mechanism operation were investigated. Tests were conducted to full-engine-power turbine speed of 45 000 rpm and to a measured drive output power level of 102 kW (137 hp). Similar drives have been parametrically tested on a back-to-back test stand to 180 kW (240 hp). Drive performance under fixed-preload operation was compared with performance under variable-roller-load operation. Comparisons were also made between the specific fuel consumption of the traction-drive-equipped engine and the original helical-gearset-equipped engine.

The traction drive was operationally compatible with the automotive gas turbine engine. The specific fuel consumption of the engine with the traction drive was comparable to that of the original helical-gear-reducer-equipped engine. Estimated peak efficiency of the traction drive based on a lubricant heat balance exceeded 92 percent. Total drive creep was 0.5 to 1.0 percentage point higher for variable-roller-load operation than for fixed. Total drive creep was always 2.5 percent or less for either system. Part-load efficiency was improved by variable-roller-load operation. Inspection of the traction rollers showed no signs of wear or surface distress.

INTRODUCTION

Prior research with the Nasvytis fixed-ratio traction drive has shown it to be a smooth, efficient power transmission (refs. 1 and 2). Two test drives, one of nominal 15:1 ratio and one of nominal 14:1 ratio, were parametrically tested on a back-to-back test stand. The former was tested to input speeds of 73 000 rpm and to input power levels of 127 kW (170 hp) (ref. 1), and the latter to 46 000 rpm and 180 kW (240 hp) (ref. 2). Peak efficiencies of 96 and 94 percent, respectively, were measured (ref. 2). Earlier Nasvytis drives have been built and tested in a number of speed and power ranges (ref. 3). These test units include a 373-kW (500-hp) reducer with a speed ratio of 48.2 and an input speed of 53 000 rpm, a 2.2-kW (3-hp), 480 000-rpm increaser with a speed ratio of 120, and a 3.7-kW (5-hp), 150 000-rpm increaser (ref. 3). All of these drives were of the multiple-row Nasvytis type with two or three rows of dual-diameter planet rollers.

One application for which high-performance, high-speed, fixed-ratio traction drives are ideally suited is the primary speed reducer for a gas turbine engine. Current developments, particularly in automotive gas turbine applications, have spurred research into quiet, efficient, compact, high-speed transmissions. State-of-the-art, twin-shaft automotive gas turbines have maximum power turbine speeds of 70 000 rpm. Designs for advanced single-shaft engines show a trend toward higher speeds, 100 000 rpm or higher, to improve efficiency and performance and to reduce size. At

these speeds the gearsets required to reduce the power turbine shaft speed to usable levels must contain small, accurate, high quality, finely pitched gears. These gears are expensive to manufacture and often difficult to cool.

Historically, traction drives have not been size competitive with gears because of the manner in which torque is transmitted. Unlike a gear mesh, a single traction contact must rely on an imposed normal load at least 10 to 20 times greater than the transmitted tangential force. However, the use of modern bearing steels, fluids with high traction coefficients, and multiple load-sharing contacts can more than offset this adverse loading situation. The steels used in earlier traction drives had significantly less fatigue resistance than today's metallurgically cleaner bearing steels. Currently, high-grade bearing steels are available that can extend the fatigue life of rolling-element systems by two to six times.

With regard to lubricants, researchers have developed synthetic hydrocarbons that can generate up to 50 percent more traction than conventional mineral oils for the same normal load (ref. 4). Because drives using these fluids can be designed for lower normal loads, service life is improved and smaller drives can be used. A 50 percent increase in traction coefficient means a 50 percent increase in torque capacity for a given life and size.

Finally in terms of design, reference 5 shows that drive size is inversely related to the number of traction elements for constant life. If a simple traction drive were designed to transmit substantial power with just two elements, much like a gearset, the element sizes would necessarily be relatively large since only one traction contact would have to transmit all of the power. To achieve high power density, a traction drive must be designed with many load-sharing rolling elements that can reduce unit loading. This has been recognized for some time. The analysis of reference 5 has shown the extent to which the drive package size and the weight-power ratio of planetary drives actually decrease as the number of planet rollers is increased for a given fatigue life. A high-performance, fixed-ratio, multicontact, simple planetary roller drive was tested over 10 years ago (ref. 6). The planetary arrangement reduced the loads on each roller and insured that the relatively large normal contact loads were internally balanced and were reacted by a ring roller rather than by bearings. Tests with this 3.5:1 ratio, six-planet-roller, 75-kW (100-hp) unit showed it to have comparable efficiency to, and substantially lower noise than, a comparable planetary gearset.

Fixed-ratio traction drives with a simple, single-row planet roller configuration are, however, limited in speed ratio range by planet-to-planet interference. The above-mentioned 75-kW design had only a 3.5:1 ratio. A remedy to the ratio and planet number limitations of simple, single-row planetary traction drives was devised by A. L. Nasvytis (ref. 3). His drive system used the sun and ring roller of the simple planetary traction drive but replaced the single row of equal-diameter planet rollers with two or more rows of "stepped" or dual-diameter planet rollers. With this new "multiroller" arrangement, practical speed ratios of 250 or higher could be obtained in a single planetary stage with one sun-roller, one ring-roller, and three planet-roller rows. Furthermore the number of planet rollers carrying the load in parallel could be greatly increased for a given ratio. This resulted in a significant reduction in individual roller contact loading, with a corresponding improvement in torque capacity, for a given fatigue life.

The high-performance, fixed-ratio Nasvytis traction drive has promise in the areas of low noise, compactness, high efficiency, and low cost. This

investigation evaluated the operational capabilities of a Nasvytis traction drive as retrofitted to an automotive gas turbine engine, compared the results with parametric data obtained on a back-to-back test stand, and compared the specific fuel consumption of the engine equipped with the traction drive to that of the original gearset-equipped engine.

The geometry typical of the Nasvytis traction (Nasvytrac) drive used in this investigation is shown in figure 1. Two rows of five stepped planet rollers are contained between the concentric high-speed sun and low-speed ring rollers. The planet rollers do not orbit. The second or outer row of planet rollers is grounded to the case through reaction bearings. This is a favorable position for the reaction bearings since the reaction forces and operating speeds are relatively low.

The sun roller and the first row of planet rollers float freely, relying on contact with adjacent rollers for location. Because of this self-supporting roller approach, the number of total drive bearings is greatly reduced and the need for the often troublesome high-speed sun roller support bearing has been eliminated. In addition, both rows of planet rollers are in three-point contact with adjacent rollers, promoting a nearly ideal internal force balance. In the event of a slight mismatch in roller loading, the first and second row of planet rollers (supported by large clearance bearings) shift under load until the force balance is reestablished. Consequently slight mismatches in roller dimensions, housing distortions under load, or thermal distortions merely cause a slight change in roller orientation without affecting performance. Because of this roller cluster flexibility, the manufacturing tolerances for roller dimensions are no more stringent than the dimensional standards set for mass-produced bearing rollers.

The number of planet-roller rows, the number of planet rollers in each row, and the relative diameter ratios at each contact are variables to be

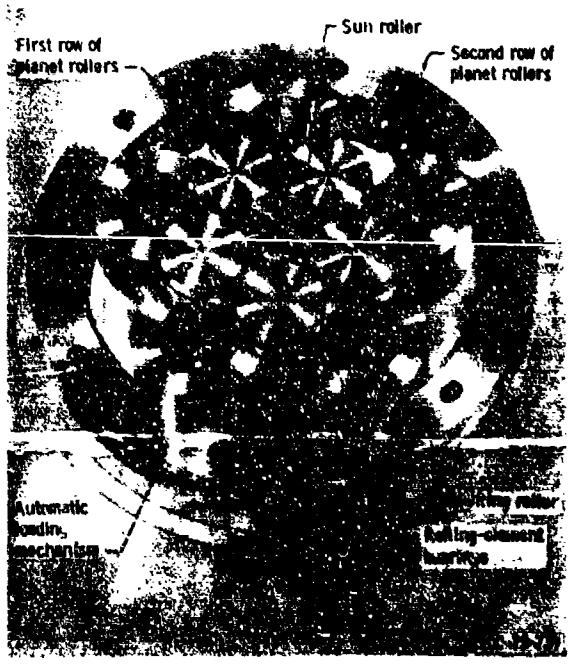

Figure 1. - Typical geometry of the Nasvytis traction drive.

optimized according to the overall speed ratio and the uniformity of contact forces. In general, drives with two planet-roller rows are suitable for speed ratios from 4 to about 35, and drives with three planet-roller rows are suitable for ratios from 10 to about 250.

In addition to the advantages of low unit loading due to multiple rollers, the elimination of high-speed bearings and numerous planet support bearings, and the high ratio capability in a single stage, the Nasvytrac drive is inherently suited for high-speed operation, often beyond that which is possible with gears. Manufacture of its cylindrically shaped rollers is relatively simple as compared with the manufacture of gear teeth. Smooth steel rollers driving through a thin lubricant film cause the drive to operate more quietly than a geared drive.

EQUIPMENT AND PROCEDURE

Test Engine

The powerplant used in this investigation was the Chrysler Corp. sixth-generation automotive gas turbine engine. This engine had been used as a baseline engine in a program that had as its goal to demonstrate an experimental gas turbine that could be competitive with the conventional internal combustion piston engine in a standard American automobile in terms of emissions, fuel economy, performance, reliability, and potential cost (ref. 7). To simplify the development, manufacture, and evaluation of critical components, the baseline engine had been designed with easily changed subassemblies. This allowed the retrofit of a traction drive speed reducer without major engine modification.

The baseline gas turbine engine is classified as a free-power-turbine, low-pressure-ratio, regenerative design. Figure 2 schematically shows the engine airflow path and major components. It basically consisted of a

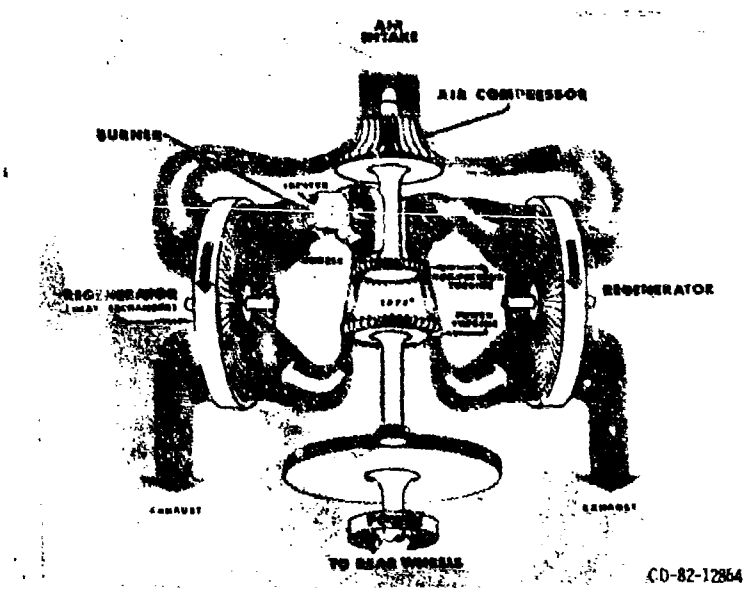

Figure 2. - Chrysler Corporation sixth generation gas-turbine engine. (Temperatures are in degrees Fahrenheit. From ref. 10.)

single-stage centrifugal compressor, a compressor turbine, variable power turbine nozzle vanes, a power turbine, two regenerators, and a helical reduction gearset. Some general descriptive data of the engine used in these tests are given in table I. Corrected engine output power and torque performance curves, based on data taken by Chrysler Corp., are shown in figure 3. The constant gas generator speed lines shown in figure 3 are roughly equivalent to a constant throttle setting. The data are presented in "corrected" form, which is based on engine operation at sea level under standard ambient conditions of 302 K (85° F) and 101 kPa (29.92 in. Hg) (ref. 8). Additional engine details can be found in reference 9.

Test Drive

The fixed-ratio, multiroller, speed reduction traction drive used in this investigation was designed to operate over the speed and power range of the gas turbine engine, with an input torque limit of 42 N-m (375 in-lbf). The drive configuration was identical to the one reported in detail in reference 2. It had speed ratios between the sun roller and first planet-roller row, between the first and second planet-roller rows, and between the second planet-roller row and the ring roller of 1.21, 3.94, and 2.93, respectively, for a nominal drive ratio of 14. The drive was equipped with an automatic roller loading mechanism incorporated into the splined high-speed coupling on the sun-roller input shaft. This mechanism adjusted the normal contact load between the rollers in proportion to the transmitted torque. The torque-responsive loading mechanism insured that sufficient normal load was applied under all conditions to prevent slip without overloading the contacts at light loads. The mechanism was designed to operate at a constant traction coefficient value of 0.05, above some preselected minimum load setting. If required, a constant level of roller normal loads could also be applied by locking the mechanism.

The ring and planet rollers were fabricated from consumable-vacuum-melted (CVM) SAE-9310 steel case carburized to a Rockwell-C hardness of 60 to 62. The sun roller was made from CVM Nitralloy 135-M steel nitrided to a similar hardness. Nitralloy was used for the sun roller because of the internal spline requirements. The roller cluster was approximately 210 mm (8.3 in.) in diameter and 60 mm (2.4 in.) wide and weighed 74.5 N (16.8 lbf).

The 14:1 ratio test drive was retrofitted into the power turbine housing in place of the engine's stock 9.69:1 ratio helical gearset. The concentric traction drive eliminated the 14-cm (5.53-in.) offset between the rotor and output shaft with the helical gear reducer. A cross section of the traction drive integrated into the engine's power turbine housing assembly is shown in figure 4 and an external view in figure 5. Removal of the gears and attachment of the sun roller to the power turbine shaft required changes to the power-turbine-shaft support bearings. In the stock engine, three radial and one thrust fluid-film bearing supported the shaft and reacted the rotor thrust and gear forces. The self-supporting sun roller of the traction drive eliminated the gear separating forces, which normally are carried by a pair of fluid-film bearings that straddle the pinion. The rear set of fluid-film bearings was replaced by a single 25-mm-diameter-bore, split-inner-race, angular-contact ball bearing mounted in an adapter block. A flexible spline coupling was designed to connect the sun roller to the power turbine shaft. The angular-contact ball bearing helped support the rotor-coupling assembly weight of 31 N (7 lbf) and also reacted the rotor thrust, which reached a maximum of 364 N (82 lbf) at full

TABLE I. - ENGINE SPECIFICATIONS

Model	A-128-1
Number	401-403
Maximum power, hp	150 at 3500 rpm
Design pressure ratio	4.1
Design airflow, lb/sec	2.29
Compressor speed (maximum), rpm	44 610
Power turbine speed (maximum), rpm	45 500
Reduction gear ratio	9.6875

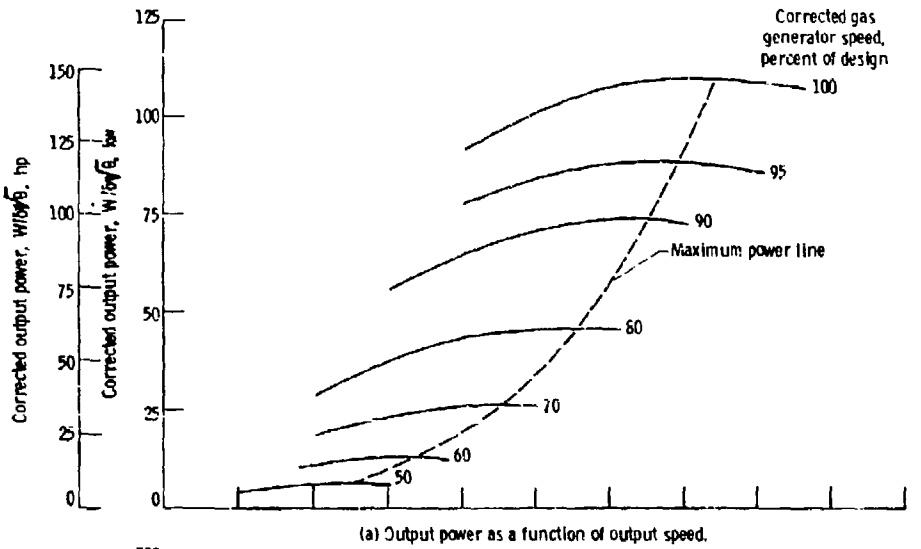

(a) Output power as a function of output speed.

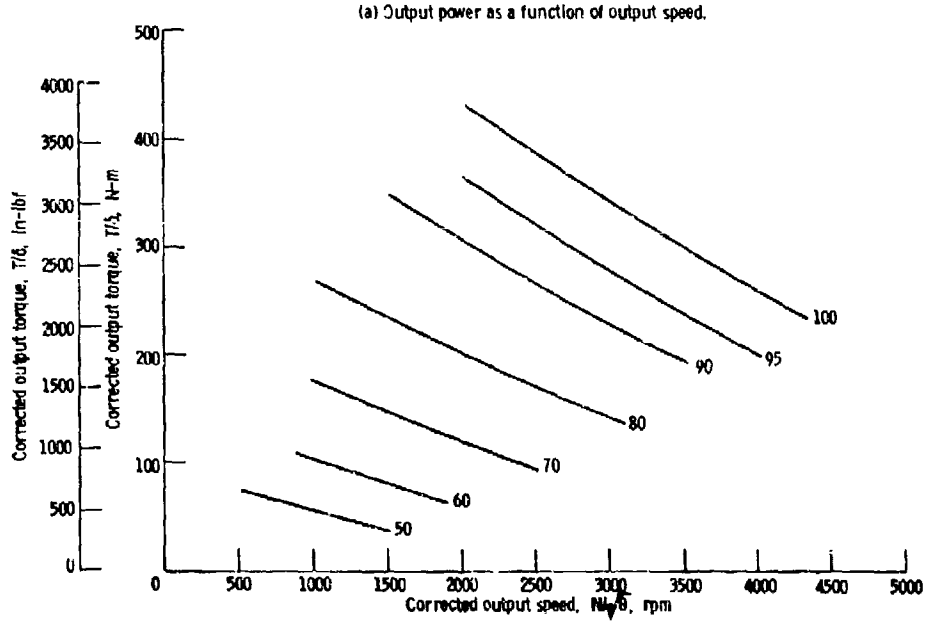

(b) Output torque as a function of output speed.

Figure 3. - Automotive gas turbine engine output characteristics with original helical gear speed reducer, based on Chrysler Corp. data, corrected to standard sea-level conditions.

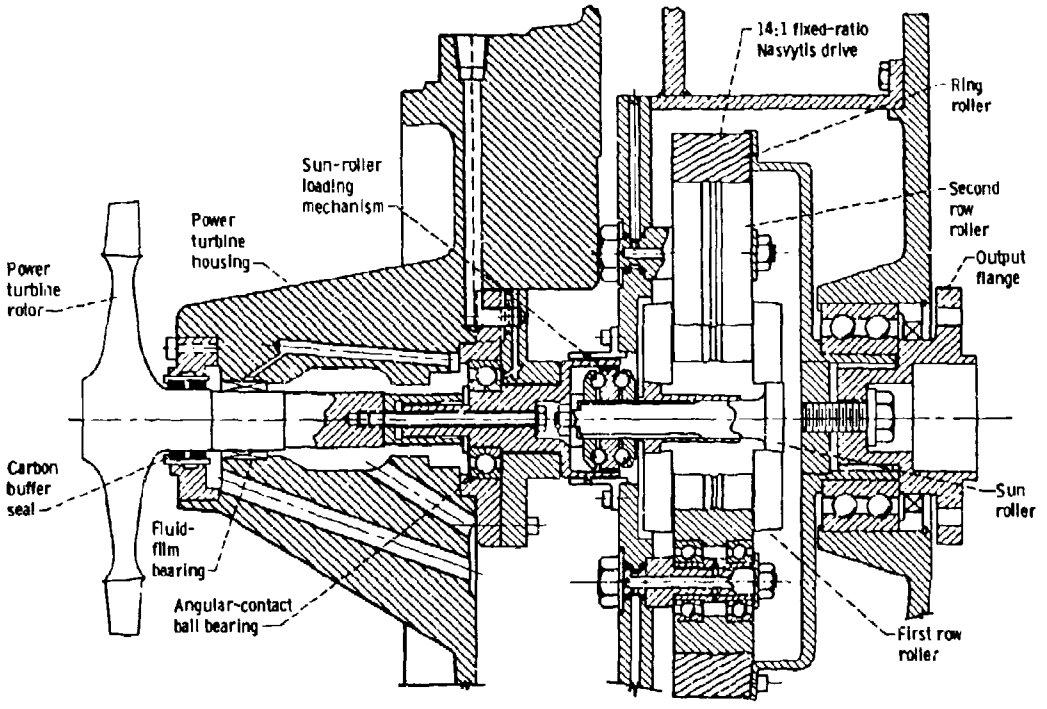

Figure 4. - Installation of the Nasvytis traction drive with power turbine assembly.

Figure 5. - Power turbine assembly. (Traction drive case shown on rear of housing.)

power. The single fluid-film bearing behind the power turbine was retained. The rotor-coupling assembly was dynamically balanced to within 0.08 g-cm (0.0015 oz-in) at these two bearing planes.

The baseline gas turbine engine was lubricated by a pump driven off the compressor (gas generator) shaft. The lubricant normally used was an automotive automatic transmission fluid. Engine lubricant in the power turbine assembly was replaced with a synthetic cycloaliphatic traction fluid that had a significantly higher coefficient of traction. Its properties are listed in table II. Lubricating not only the traction drive but also the power turbine support bearings eliminated a potential sealing problem. The effect of the lubricant change on the remaining fluid-film bearing was judged to be insignificant because of the similarity in the kinematic viscosities of the automatic transmission fluid (7.0×10^{-6} m^2/sec at 372 K) and the test traction lubricant (5.5×10^{-6} m^2/sec at 372 K).

Test Stand

The NASA automotive gas turbine test stand used in this investigation permits steady-state parametric testing and performance mapping with an eddy-current dynamometer power absorber. The test engine installed on the stand is shown in figure 6. The traction drive housing and two large exhaust ducts that straddle the engine are visible. Intake air, an exhaust duct system, an oil cooler, a starting battery, and a multiple-fuel system are provided. Engine output is directly connected via a drive shaft to the power absorber. Output torque is measured with a torque arm and a load cell on the cradled dynamometer. Speed is determined by a magnetic pickup on a toothed wheel. Gas turbine engine instrumentation is designed for measurement of specific fuel consumption and engine operational temperature and pressure data. The traction drive lubrication system consisted of a 0.019-m^3 (5-gallon) sump, a pressure pump, an oil heater and cooler, a 3-?m absolute supply line filter, separate flow control valves for the traction drive inlet and the power turbine bearings inlet, and two scavenge pumps to keep the drive housing and the power turbine housing relatively dry.

Power losses from the traction drive and the power turbine bearings were each determined approximately by a heat balance technique. Temperatures of the oil inlet and outlet streams of both the power-turbine-shaft bearings and the traction drive were recorded. Input oil temperatures were maintained constant by automatic control. Lubrication flow rates were measured by turbine flowmeters. Speeds were accurately measured to one part in ten thousand with a proximity probe and magnetic pickups on the power turbine and drive output shafts. This allowed accurate measurement of creep and its effect on the overall drive ratio. Creep is the slight inherent relative motion between driving and driven rollers in a traction drive under torque transfer. Details of the creep calculation can be found in reference 1.

Critical component temperatures were measured by thermocouples. Sun roller temperatures in the test drive were obtained approximately with a thermocouple junction placed 3 mm (0.1 in.) from the roller surface. Thermocouples inbedded in copper plugs were used to measure the inner race temperatures of the second row of planet bearings and the outer race temperatures of the output-shaft double-row ball bearing and the power-turbine-shaft angular-contact ball bearing. Similar thermocouple plugs were placed inside the cast power turbine housing in contact with the

TABLE II. - PROPERTIES OF SYNTHETIC CYCLOALIPHATIC TRACTION LUBRICANT

Additives	Antiwear[a]; oxidation inhibitor; antifoam; viscosity index improver[b]
Kinematic viscosity, cm^2/sec, at-	
244 K (-20° F)	$41\ 500 \times 10^{-2}$
311 K (100° F)	34×10^{-2}
372 K (210° F)	5.6×10^{-2}
Flashpoint, K; °F	435; 325
Fire point, K; °F	447; 345
Autoignition temperature, K; °F	600; 620
Pour point, K; °F	236; -35
Specific heat at 311 K (100° F), J/kg-K; Btu/lb-°F	2130; 0.51
Thermal conductivity at 311 K (100° F), J/m-sec-K; Btu/hr-ft-°F	0.10; 0.060
Specific gravity at 311 K (100° F)	0.889

[a]Zinc dialkyl dithlophosphate.
[b]Polymethacrylate.

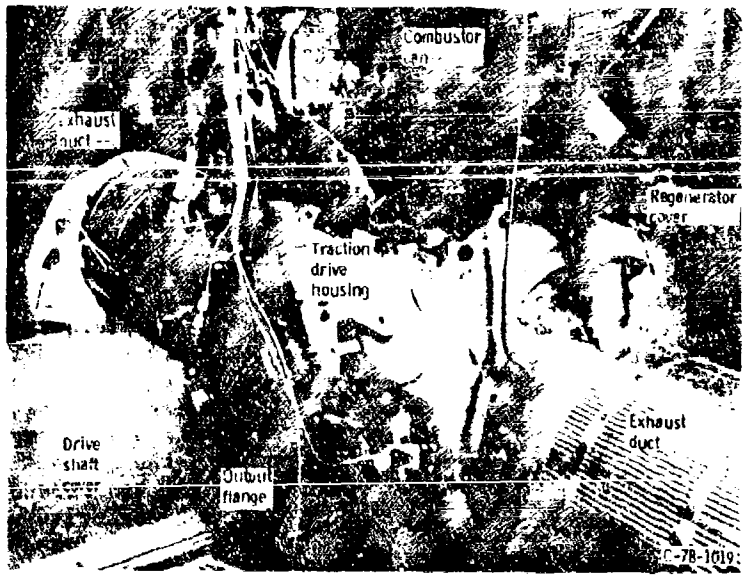

Figure 6. - Traction-drive-equipped engine on NASA engine test stand.

power-turbine-shaft journal bearing sleeve and the carbon-buffer-seal support housing. Test drive outside skin temperatures were also measured.

To determine the effectiveness of the roller loading mechanism, an eddy-current proximity probe was used to monitor sun-roller axial position. Turbine shaft rotor dynamics were sensed by orthogonal, radial proximity probes at three locations (between the journal bearing and buffer seal, near the center of the shaft, and on the maximum diameter of the coupling) and were monitored by using an oscilloscope.

The automatic data acquisition and retrieval system collected temperature, pressure, flow, speed, and torque data from the gas turbine engine and traction drive. At each operating point where data were recorded, five readings were taken over a period of several seconds and then averaged.

Test Procedure

A spin test was conducted to check out the integrated traction drive and modified turbine shaft support system assembly and to isolate any rotor dynamics problems before committing the test hardware to the engine cell. The rotor and the power turbine housing containing the drive were mounted in open air and driven backward from the low-speed output shaft to rotor speeds of 21 000 rpm and power levels of 15 kW (20 hp). During this test the automatic roller loading mechanism was locked out and a constant preload equal to approximately 76 percent of the design maximum was set.

Upon successful completion of the checkout spin tests, two series of parametric tests of the gas turbine engine - traction drive assembly were run on the engine dynamometer stand: a fixed-preload test series where the roller loading mechanism was locked at a constant (near maximum) roller normal load and a variable-roller-load test series. The testing sequence was to maintain a constant (dynamometer controlled) output speed and then to increase torque in stepwise manner by adjusting the engine throttle setting. To insure steady-state conditions in the engine and drive, 10 to 15 minutes of running was allowed after speed changes and 5 to 10 minutes after torque changes before a data point was recorded. The range of operating points for the engine with traction drive was somewhat limited by the test stand. Since the engine test cell dynamometer was initially sized for the gas turbine engine with its original helical gearset reducer, substitution of the traction reducer with a 45 percent greater speed reduction ratio resulted in output torques at low speeds that exceeded the torque capacity of the dynamometer. Thus some of the high-torque, low-speed engine operating points could not be obtained with the existing system.

The fixed-preload test was conducted to check out the engine drive interactions with a simplified (no loading mechanism) traction drive system. On the basis of back-to-back stand tests of the drive components (ref. 2) the constant preload was set at 76 percent of the maximum possible roller load, and the maximum torque allowed in this test was chosen accordingly. The total lubricant flow rate to the traction drive was set at 0.13 liter/sec (2.0 gallon/min), and the power turbine journal and ball bearings received 0.04 liter/sec (0.6 gallon/min). The inlet temperatures on both streams were 328 K (130° F). Maximum output torques of 407, 373, 407, and 244 N-m (3600, 3300, 3600, 2100 in-lbf) were achieved at output shaft speeds of 800, 1600, 2400, and 3150 rpm, respectively.

After a successful fixed-preload test the roller loading mechanism was reactivated. Minimum roller load was set at 27 percent of maximum in order to insure positive roller contact at light loads and high speeds. The lubricant flow rates were the same as in the fixed-preload tests. Lubricant inlet temperatures were set at 339 K (150° F). Maximum output torques of 407, 475, 407, and 271 N-m (3600, 4200, 3600, 2400 in-lbf) were reached at output shaft speeds of 800, 1600, 2400, and 3150 rpm, respectively.

A set of tests was run on the engine with the original helical gearset reinstalled for comparison. To make a reasonable performance comparison, test points for the gearset test were chosen to correspond to the same gas

generator speed and power turbine speed points recorded during the variable-roller-load parametric tests. For all tests the engine oil inlet temperature was 339 K (150° F).

RESULTS AND DISCUSSION

Traction Drive Performance

The drive and power turbine rotor assembly spin test was not intended to produce steady-state temperature data. Critical temperatures were monitored, however, and generally showed a gradual increase with speed. Orthogonal proximity probes located on the turbine rotor between the buffer seal and the fluid-film bearing measured a maximum total runout of 0.038 mm (0.0015 in.) at low speed. At higher speeds, above 8000 rpm, the maximum was 0.025 mm (0.001 in.) except near 10 000 rpm, where the oscilloscope indicated an excursion of 0.045 mm (0.0018 in.). This runout was within the static diametral clearance in the journal bearing, which was measured prior to the test to be about 0.076 mm (0.003 in.). The excursion at 10 000 rpm quickly disappeared as speed was increased, suggesting that it was a system "critical" that would be readily kept in check by the damping provided by the front journal bearing. Maximum coupling runout was 0.076 mm (0.003 in.). Since the spin test was successful, no changes in the test hardware were necessary.

The effect of output speed and torque on the power losses of the traction drive and the power-turbine-shaft bearings is shown in figure 7 for the two parametric engine drive test series. As stated earlier in this report the power loss is based on the amount of heat rejected to the lubricant as determined by a heat balance of each inlet and outlet oil stream. This heat balance technique is considered to give approximate results. No attempt was made to quantify the heat convected to the atmosphere through the drive casting or that to the lubricant from the hot engine components or the possible small temperature rise due to throttling through small passageways.

Figure 7(a) shows that, when operating in a fixed-preload mode, the traction drive power loss was weakly dependent on torque and strongly dependent on speed. In figure 7(b) the effect of speed on power loss was also very strong for the variable-roller-load operation, but the power loss increased much faster with torque. Comparing figures 7(a) and (b) shows that the power loss for the variable-roller-load operation was significantly less at low torques because of the reduced roller normal loads. This resulted in improved part-load efficiency and extended fatigue life. At higher torques the power losses for both systems tended to reach the same levels as the roller normal loads approached similar values.

Some differences in the absolute power loss levels of figures 7(a) and (b) were caused by the difference in inlet lubricant temperature. Initially it was set at 328 K (130° F) to maximize the traction lubricant's available traction coefficient, which is known to decrease with temperature. For the variable-roller-load tests, the inlet temperature was increased to 339 K (150° F) in order to reduce power losses and to permit direct comparison with the original, gear-equipped engine, whose oil inlet temperature was also 339 K (150° F). Figure 7(b) shows the effect of lubricant inlet temperature on traction drive power loss at one engine condition (339-N-m (3000-in-lbf) output torque and 1600-rpm output speed) during the variable-roller-load tests. Data were taken approximately 7 minutes after

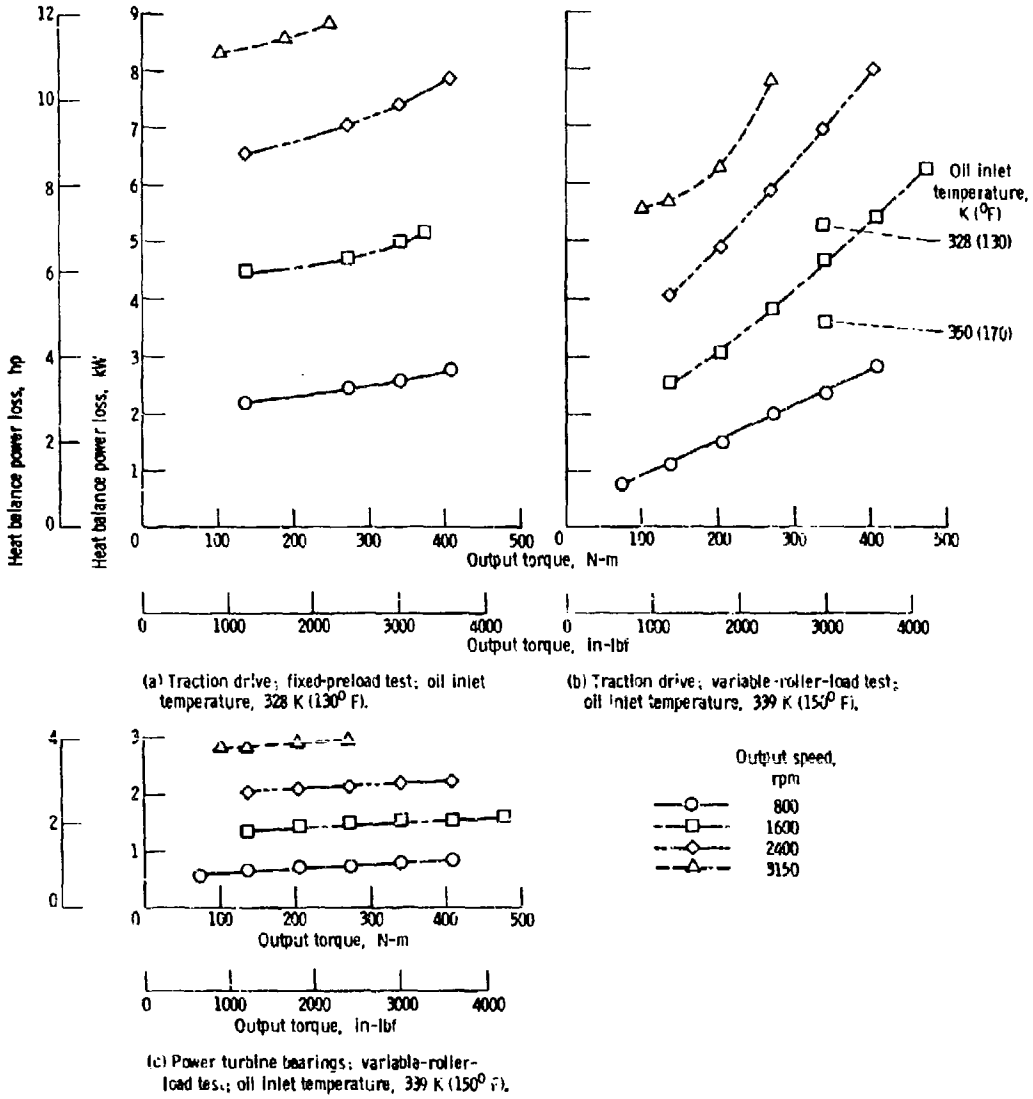

(a) Traction drive; fixed-preload test; oil inlet temperature, 328 K (130° F).

(b) Traction drive; variable-roller-load test; oil inlet temperature, 339 K (150° F).

(c) Power turbine bearings; variable-roller-load test; oil inlet temperature, 339 K (150° F).

Figure 7. - Heat balance power loss as a function of output torque and output speed. Power loss calculated from heat rejected to lubricant.

the inlet temperature was dropped from 339 K (150° F) to 328 K (130° F) and also after the temperature was raised from 328 K (130° F) to 350 K (170° F) to provide steady-state readings while the engine operating conditions were held constant. Higher inlet temperatures decreased the power loss, while lower inlet temperatures increased the power loss. This is similar to many other mechanical components, such as gears and bearings, which exhibit reduced losses at higher operating temperatures.

Figure 7(c) shows that the heat balance power loss of the power-turbine-rotor support bearings was relatively insensitive to output torque and approximately linear with speed, ranging from an average of 0.75 kW (1.0 hp) at 800-rpm output speed to 2.9 kW (3.9 hp) at 3150 rpm. Although only the data from the varaible-roller-load tests are shown, the

power-turbine bearing losses were nearly identical for the fixed-preload and variable-roller-load tests at any given output speed and torque condition.

Estimated traction drive efficiencies and power turbine bearing efficiencies for the fixed-preload and variable-roller-load test runs are shown in figure 8. These efficiencies were calculated from the measured output shaft power and the two heat balance power losses. As would be expected the efficiency of the fixed-preload drive was lower than that of the variable-roller-load drive at part-load conditions, as shown in figure 8(c), which is a comparison of the data of figures 8(a) and (b). The efficiencies of both systems merge at higher torques, reaching a maximum of over 92 percent for each test series. The bands of traction drive efficiency reflect a very small dependence on speed, with the higher efficiencies generally occurring at low output speeds at a given output torque. Power turbine bearing efficiency was virtually independent of speed. Also shown in figure 8(c) is the average efficiency of the traction drive (as a speed reducer) measured on the back-to-back test stand reported in reference 2, over the range of engine test speeds. Fairly good agreement was obtained between the stand-measured efficiency and that determined from heat balances on the lubricant in the engine tests.

The effect of operating torque and speed on traction drive creep rate is presented in figure 9. Also included for comparison are the back-to-back data (ref. 2) from the sun-loader reducer drive at 2500-rpm output speed. The agreement between both sets of creep data is within 0.2 percentage point at all corresponding test speeds (not shown in fig. 9) except at 3150-rpm output speed, where the stand measurements indicated about 0.5 percentage point greater creep rate than the engine test data at the higher torque levels.

Traction force versus creep rate curves for constant normal load generally rise linearly with transmitted torque until the maximum available traction coefficient of the lubricant is approached. At this point the creep rate begins to increase rapidly. When the maximum available traction coefficient is reached, creep changes to impending gross slip. The upward curved trend of the fixed-preload creep data of figure 9 suggests that this condition was being approached. On the other hand the variable-roller-load curves, though at a somewhat higher level due to lower normal loads, showed a tendency to level off. This is indicative of the roller loading mechanism holding a nearly constant traction coefficient.

Creep rate represents a loss in speed and thus a power loss. The lower creep rate of about 0.6 percentage point associated with fixed-preload operation was due to the higher roller normal loads. This lowered the applied traction coefficient so that the resulting creep rate was relatively small. However, as mentioned previously, the overall efficiency was inferior to that of variable-roller-load operation (fig. 8) because of the losses associated with contact overloading. Also, the creep rate in figure 9 at a given torque was lowest for the lowest output speed under either fixed or variable loading. The reason was the deleterious effect of traction element surface speed on available lubricant traction coefficient and creep rate at a given load. This helps to explain why the drive exhibited greater efficiency at the lower operating speeds in the efficiency bands of figure 8.

The axial position of one side of the two-piece sun roller assembly as monitored by a proximity probe is shown in figure 10. In this drive, as the tapered sun-roller halves moved together, the normal load on the roller cluster was correspondingly increased. During the variable-roller-load test, as shown in figure 10, the sun-roller halves moved inward together in

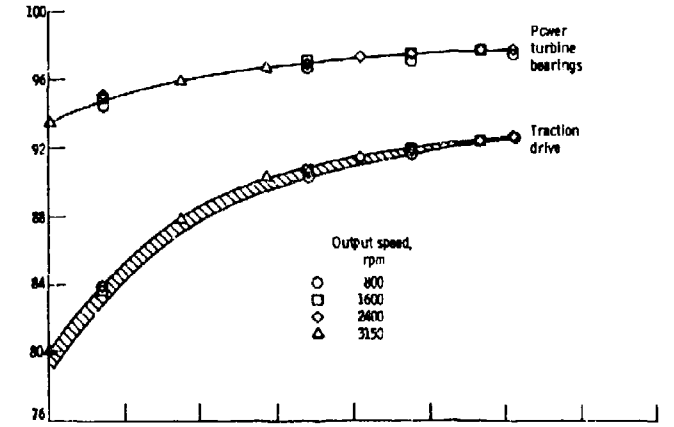

(a) Fixed-preload test; oil inlet temperature, 328 K (130° F).

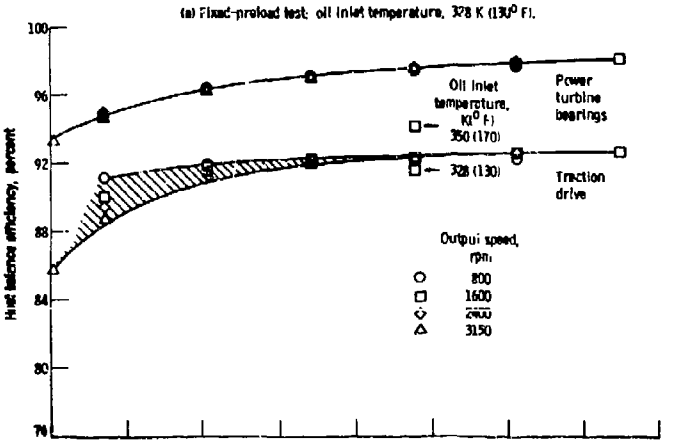

(b) Variable-roller-load test; oil inlet temperature, 339 K (150° F).

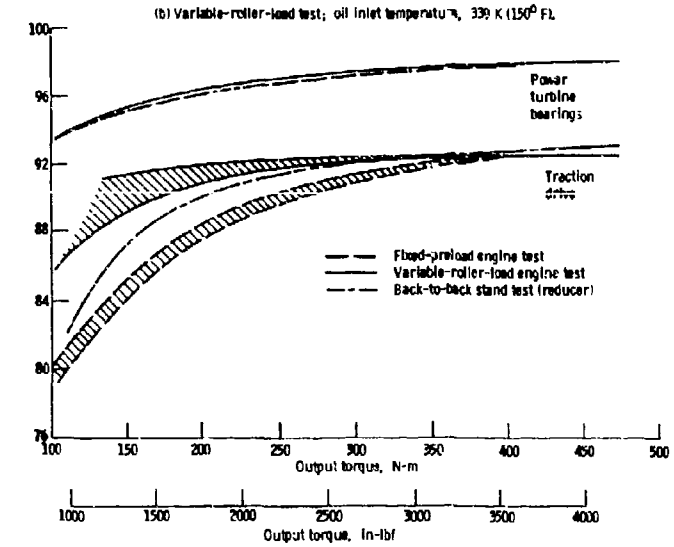

(c) Comparison of fixed-preload engine test, variable-roller-load engine test, and back-to-back variable-roller-load test.

Figure 8. - Heat balance efficiency of the traction drive and the power turbine bearings as a function of output torque and output speed.

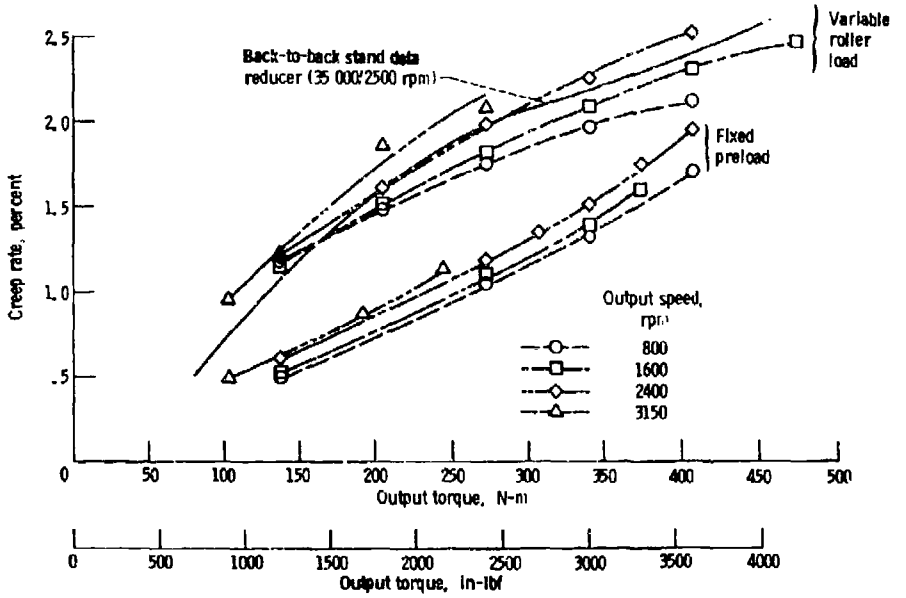

Figure 9. - Creep rate as a function of output torque and output speed for fixed-preload and variable-roller-load tests.

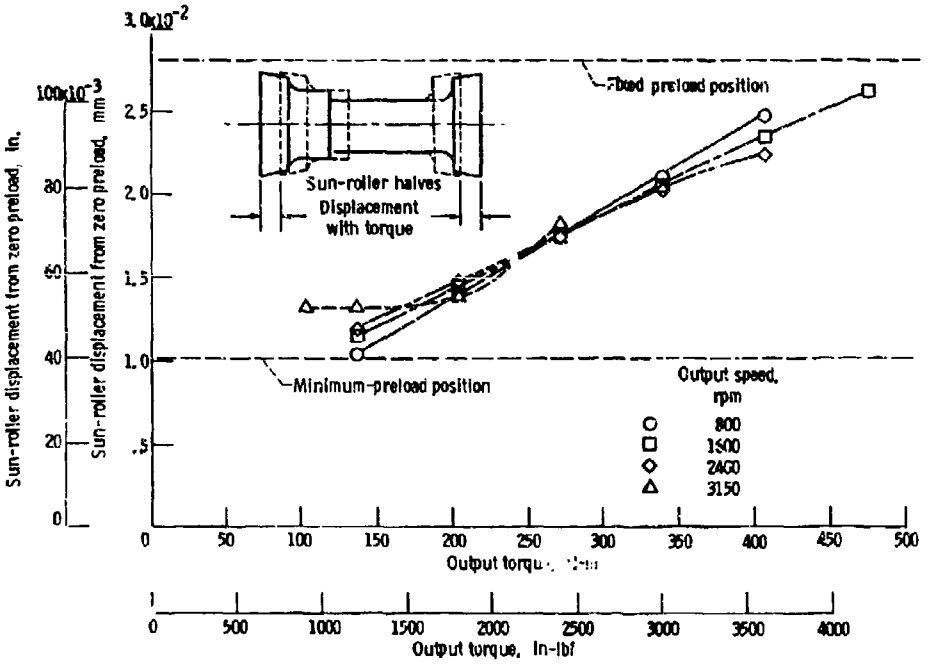

Figure 10. - Sun-roller displacement as a function of output torque and output speed; variable-roller-load test.

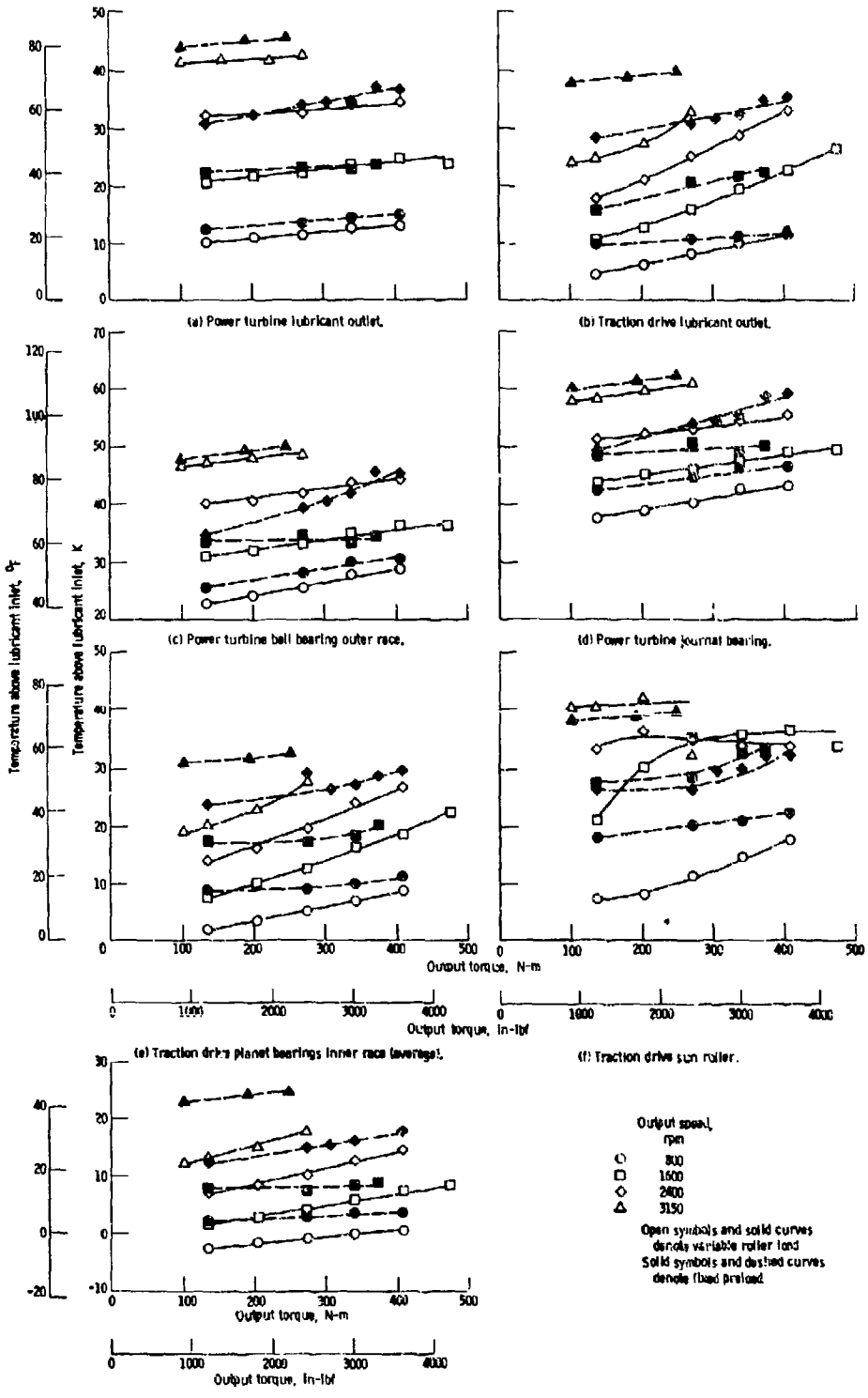

Figure 11. - Traction drive and power turbine assembly component temperatures as a function of output torque and output speed; fixed-preload and variable-roller-load tests.

a nearly linear fashion with increasing torque, indicating satisfactory roller loading action. Because of centrifugal force effects on the loading balls, an increase in speed caused a slight increase in initial preload. The loading mechanisms on both the speed increaser and reducer sun-loading back-to-back test stand units showed similar behavior.

All measured temperatures of the roller elements in the traction drive increased with an increase in operating speed, as shown in figure 11. Generally the operating temperature rise above the lubricant inlet temperature was greater in the fixed-preload test than in the variable-roller-load test. The sun-roller temperature, as measured by a thermocouple near the surface, was the highest in the drive. Tests on the back-to-back stand indicate that this approximate sun-roller temperature tended to fluctuate much more than that of the other components. Sun-roller temperatures for both the fixed-preload and variable-roller-load tests never exceeded 42 K (76° F) above the respective lubricant inlet temperature. Traction drive component temperatures were very close to those from the back-to-back stand data (ref. 2). Power turbine bearing temperatures also increased with speed. Fixed-preload readings in terms of temperature rise above lubricant inlet temperature were slightly higher than corresponding variable-roller-load readings.

In general the Nasvytis drive demonstrated operational compatibility with the gas turbine engine and smooth performance throughout the engine's torque and speed range. Orthogonal, radial proximity probes showed that the coupled rotor-traction drive system was reasonably stable from engine idle to maximum speed. Maximum coupling runout reached 0.127 mm (0.005 in.) at 3150 rpm in the variable-roller-load tests. Peak-to-peak rotor motion measured near the front journal bearing is shown in figure 12 for the variable-roller-load tests. A half-frequency whirl was encountered while changing output speed from 2400 rpm to 3150 rpm at approximately 35 000-rpm power turbine speed. This was observed on the oscilloscope as a limiting orbit condition where there was no further growth beyond an eccentricity of 0.018 mm (0.0007 in.). In all cases the peak-to-peak runout was within the measured static diametral clearance of the front journal bearing.

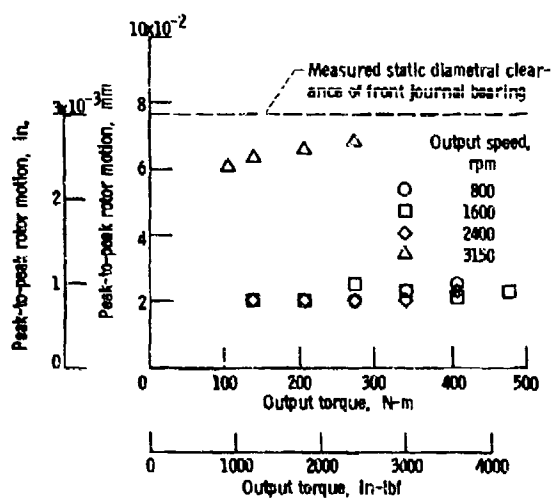

Figure 12. - Peak-to-peak power turbine rotor motion as a function of output torque and output speed; variable-roller-load test.

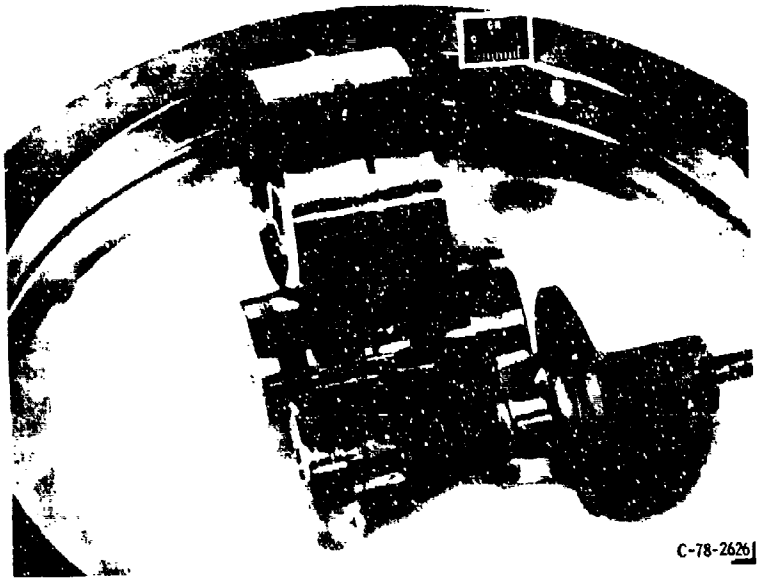

Figure 13. - Traction drive rollers after completion of engine testing.

Total test stand operational time of the traction-drive-equipped engine was 10.2 hours. Upon completion of the tests the drive was disassembled and inspected for wear and surface distress. Figure 13 shows the sun, ring, and typical planet rollers after the tests. The original grinding marks are still visible, with no signs of wear or distress. Some light, circumferential scratches were evident, presumably from small debris particles. Such scratches are commonly found on rollers in roller bearings after the same period of service.

Engine Performance

Fuel flow measurements and specific fuel consumption calculations were made at each test point in both the traction drive and gearset tests. Figure 14 shows the specific fuel consumption (sfc) as a function of gas generator speed for three power turbine speeds from the gearset and variable-roller-load tests. In this plot, the values of sfc and gas generator speed are corrected values, but those for power turbine speed are not. Although the traction drive output speed was dynamometer controlled, the power turbine speed varied slightly with torque because of the variable creep rate. Thus the power turbine speeds shown in figure 14 are nominal speeds. To make a fair comparison of engine performance between the engine with the gearset and that with the traction drive, power turbine and gas generator speeds were chosen for the gearset test so that the operating conditions of the engine itself (not including the speed reducer) would be equivalent.

Figure 14 shows that the sfc for the traction-drive-equipped engine was very close to the sfc for the gearset-equipped engine. For most engine operating points at 23 000- and 35 000-rpm power turbine speed, the traction-drive-equipped engine sfc was equal to or less than the gearset-equipped engine sfc. At 12 000-rpm power turbine speed, and at

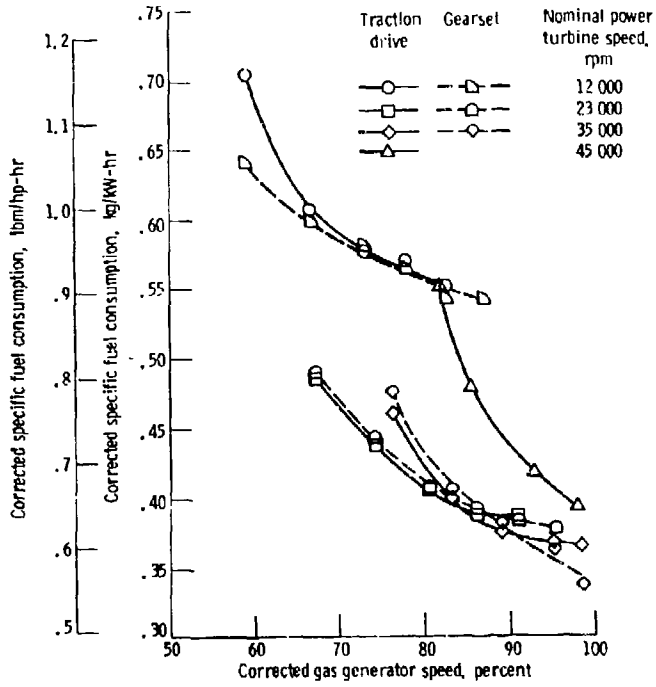

Figure 14. - Engine specific fuel consumption as a function of gas generator speed and power turbine speed for engine with original helical gearset and with variable-roller-load traction drive.

35 000-rpm power turbine speed between 90 and 100 percent gas generator speed, the traction-drive-equipped engine sfc ranged from less than 1 percent to 10 percent greater than that of the gearset-equipped engine.

The usual testing procedure for performance characterization on the automotive gas turbine test stand is to hold gas generator speed constant and vary output speed, taking data at numerous points including the maximum power point for each gas generator speed. The curves in figure 3 were produced in this way. By using this method a performance plot of sfc against gas generator speed at maximum power can be plotted directly. Since the test procedure used in the traction drive tests held output speed constant and varied gas generator speed, the data from figure 14 were first cross-plotted as sfc against nominal power turbine speed with lines of constant gas generator speed. Then the points of maximum power for each gas generator speed were identified in terms of power turbine speed, based on the data of an earlier engine test (fig. 3(a)). The sfc for each of these maximum power points can then be plotted against gas generator speed as in figure 15. This figure shows that the sfc of the engine with the variable-roller-load traction drive speed reducer was comparable to the sfc of the original helical-gearset-equipped engine. At 100 percent gas generator speed, the traction-drive-equipped engine exhibited an sfc of 0.36 kg/kW-hr (0.59 lbm/hp-hr), while the sfc of the engine with gearset was 0.35 kg/kW-hr (0.58 lbm/hp-hr).

It should be pointed out that, though all these tests were run on the same basic engine, there were some minor differences between the traction-drive-equipped engine and the gearset-equipped engine apart from the obvious difference in speed reducer ratio and power turbine support bearings. First, different power turbine rotors and power turbine

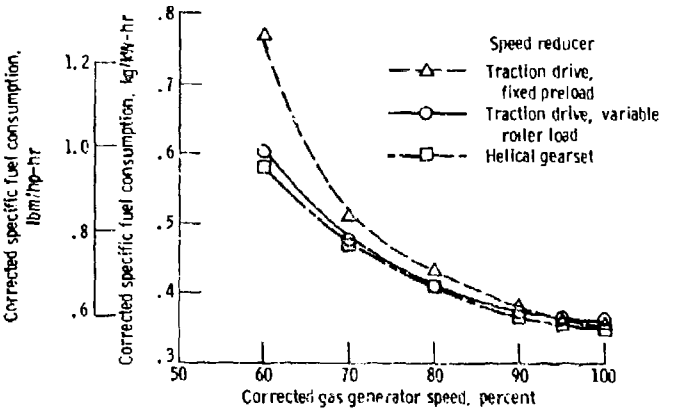

Figure 15. - Comparison of engine specific fuel consumption at maximum power as a function of gas generator speed for traction and gear speed reducers. (Points shown are cross plotted.)

assemblies of the same design were used. Differences in housing assembly - engine buildup can cause variations in power turbine blade tip-to-shroud clearance that can affect power turbine performance. Second, a variable inlet guide vane assembly was installed in the baseline engine after the traction drive tests for future engine component tests. This assembly was left in place with vanes set at zero degrees for the gearset test. Minor effects on engine performance might have been produced by the presence of the vane assembly. These include a performance loss due to a small pressure drop across the vanes and a performance gain due to inlet guidance by the vanes. Third, the lubrication systems were different. In the gearset-equipped engine, all of the bearings were lubricated by a pump driven off the gas generator shaft. For the traction-drive-equipped engine an external, constant-flow system supplied lubricant to the traction drive and the power turbine support bearings. Other test differences were possible engine component erosion from extensive water injection tests between the traction drive and gearset tests and the use of different batches of the same type of diesel fuel.

SUMMARY OF RESULTS

Parametric tests were conducted on a 14:1 fixed-ratio Nasvytis multiroller traction drive speed reducer retrofitted to an automotive gas turbine engine. The traction drive's sun-roller assembly was equipped with an automatic roller loading mechanism. Modifications to the gas turbine engine's power turbine assembly were made to accommodate the planetary configuration traction drive in place of the offset, 9.69:1 ratio helical gearset. A synthetic, cycloaliphatic traction fluid was used to lubricate both the traction drive and the power turbine support bearings. The effects of speed and torque on drive power loss, efficiency, creep rate, temperature distribution, and loading mechanism action were investigated. Tests were conducted to a full-engine-power turbine speed of 45 000 rpm and to a measured drive output power level of 102 kW (137 hp). Comparisons were made with drive performance data that had been generated on a back-to-back test stand to 180 kW (240 hp). Drive performance under fixed-preload operation was compared with performance under variable-roller-load operation. Comparisons were also made between the specific fuel consumption of the

traction-drive-equipped engine and that of the original gearset-equipped engine. The following results were obtained:

1. The drive showed good operational compatability with the automotive gas turbine engine.

2. Specific fuel consumption of the engine with the traction drive speed reducer installed was comparable to that of the original helical-gearset-equipped engine.

3. Estimated peak efficiency of the traction drive based on a lubricant heat balance exceeded 92 percent.

4. Total drive creep was higher for variable-roller-load operation. It was always less than or equal to 2.5 percent.

5. Part-load efficiency was higher for variable-roller-load operation.

6. Post-test inspections of the traction roller surfaces showed no signs of wear or surface distress.

National Aeronautics and Space Administration
Lewis Research Center
Cleveland, Ohio, January 25, 1982

REFERENCES

1. Loewenthal, Stuart H.; Anderson, Neil E.; and Nasvytis, A. L.: Performance of a Nasvytis Multiroller Traction Drive. NASA TP-1378, AVRADCOM-TR-78-36, 1978.

2. Loewenthal, S. H.; Anderson, N. E.; and Rohn, D. A.: Evaluation of a High Performance Fixed-Ratio Traction Drive. J. Mech. Des., vol. 103, no. 2, Apr. 1981, pp. 410-422.

3. Nasvytis, A. L.: Multiroller Planetary Friction Drives. SAE Paper 660763, Oct. 1966.

4. Green, R. L.; and Langenfeld, F. L.: Lubricants for Traction Drives. Mach. Des., vol. 46, no. 11, May 1974, pp. 108-113.

5. Rohn, D. A.; Loewenthal, S. H.; and Coy, J. J.: Simplified Fatigue Life Analysis for Traction Drive Contacts. J. Mech. Des., vol. 103, no. 2, Apr. 1981, pp. 430-439.

6. Hewko, L. O.: Roller Traction Drive Unit for Extremely Quiet Power Transmission. J. Hydronaut., vol. 2, no. 3, July 1968, pp. 160-167.

7. Baseline Gas Turbine Development Program. COO-2749-T1, Dept. of Energy, 1973.

8. Gas Turbine Engine Test Code. SAE Handbook, SAE Recommended Practice SAE J116a, Society of Automotive Engineers, Inc., 1978, pp. 24.26-24.28.

9. Wagner, C. E.; and Pampreen, R. C., eds.: Baseline Automotive Gas Turbine Engine Development Program. (Chrysler Corp.; DOE Contract EY-76-C-02-2749.) DOE/NASA/2749-79/1, vol. 1, NASA CR-159670, 1979. (also COO-2749-42)

10. Summary Report of Fourth Automotive Power Systems Contractors Coordination Meeting, Ann Arbor, Mich., Dec. 12-15, 1972.

1. Report No.	2. Government Accession No.	3. Recipient's Catalog No.
NASA TP-2027 AVRADCOM TR 81-C-11	A D- A 1 1 6 7 0 8	

4. Title and Subtitle	5. Report Date
MULTIROLLER TRACTION DRIVE SPEED REDUCER - EVALUATION FOR AUTOMOTIVE GAS TURBINE ENGINE	June 1982
	6. Performing Organization Code 511-58-12
7. Author(s) Douglas A. Rohn, Neil E. Anderson, and Stuart H. Loewenthal	8. Performing Organization Report No E-1002
	10. Work Unit No.
9. Performing Organization Name and Address National Aeronautics and Space Administration Lewis Research Center Cleveland, Ohio 44135	11. Contract or Grant No
	13. Type of Report and Period Covered Technical Paper
12. Sponsoring Agency Name and Address National Aeronautics and Space Administration Washington, D.C. 20546	14. Sponsoring Agency Code

15. Supplementary Notes

Douglas A. Rohn, Lewis Research Center; Neil E. Anderson, AVRADCOM Research and Technology Laboratories; Stuart H. Loewenthal, Lewis Research Center.

16. Abstract

Tests were conducted on a nominal 14:1 fixed-ratio Nasvytis multiroller traction drive retrofitted as the speed reducer in an automotive gas turbine engine. Power turbine speeds of 45 000 rpm and a drive output power of 102 kW (137 hp) were reached. The drive operated under both variable roller loading (proportional to torque) and fixed roller loading (automatic loading mechanism locked). The drive operated smoothly and efficiently as the engine speed reducer. Engine specific fuel consumption with the traction speed reducer was comparable to that with the original helical gearset.

17. Key Words (Suggested by Author(s))	18. Distribution Statement
Traction drives; Transmissions; Traction; Drives; Gas turbine drive; Speed reducers	Unclassified - unlimited STAR Category 37

19. Security Classif. (of this report)	20. Security Classif (of this page)	21. No. of Pages	22. Price*
Unclassified	Unclassified	23	A02

* For sale by the National Technical Information Service, Springfield, Virginia 22161

NASA-Langley, 1982